



Published in final edited form as:

Sens Actuators B Chem. 2016 November 1; 235: 126–135. doi:10.1016/j.snb.2016.05.010.

An Efficient Power Harvesting Mobile Phone-Based Electrochemical Biosensor for Point-of-Care Health Monitoring

Alexander C. Sun¹, Chengyang Yao¹, A. G. Venkatesh¹, and Drew A. Hall^{1,*}

¹Department of Electrical and Computer Engineering, University of California, San Diego, La Jolla, CA, USA

Abstract

Cellular phone penetration has grown continually over the past two decades with the number of connected devices rapidly approaching the total world population. Leveraging the worldwide ubiquity and connectivity of these devices, we developed a mobile phone-based electrochemical biosensor platform for point-of-care (POC) diagnostics and wellness tracking. The platform consists of an inexpensive electronic module (< \$20) containing a low-power potentiostat that interfaces with and efficiently harvests power from a wide variety of phones through the audio jack. Active impedance matching improves the harvesting efficiency to 79%. Excluding losses from supply rectification and regulation, the module consumes 6.9 mW peak power and can measure < 1 nA bidirectional current. The prototype was shown to operate within the available power budget set by mobile devices and produce data that matches well with that of an expensive laboratory grade instrument. We demonstrate that the platform can be used to track the concentration of secretory leukocyte protease inhibitor (SLPI), a biomarker for monitoring lung infections in cystic fibrosis patients, in its physiological range via an electrochemical sandwich assay on disposable screen-printed electrodes with a 1 nM limit of detection.

Keywords

smartphone; mHealth; point-of-care; electrochemical biosensor; audio jack; power rectification

1. Introduction

Explosive growth in the mobile market over the last few decades have made cellular phones internationally ubiquitous, with approximately 7 billion subscribers worldwide [1]. This dependence on cell phones both in the developing world, where older multi-functionality phone models dominate, and in highly developed nations, where roughly 2.03 billion smartphones are being currently used, has created a highly dispersed, yet interconnected infrastructure of mobile technology [2]. Hence, due to the widespread availability and the continual advancement of electronics, these pervasive devices have begun to function as

* drewhall@ucsd.edu.

Publisher's Disclaimer: This is a PDF file of an unedited manuscript that has been accepted for publication. As a service to our customers we are providing this early version of the manuscript. The manuscript will undergo copyediting, typesetting, and review of the resulting proof before it is published in its final citable form. Please note that during the production process errors may be discovered which could affect the content, and all legal disclaimers that apply to the journal pertain.

more than just phones. By adding peripheral sensors, these devices can enable a wide variety of auxiliary applications spanning from mobile payment and banking to fitness and health tracking. The main advantage of these peripherals is that by leveraging the powerful functionality already available on mobile phones, more advanced and portable systems can be implemented that are often more accessible, cost-effective, and practical than equivalent specialized tools, such as the case with the Square credit card reader dongle, the iBGStar® blood glucose meter, and the AliveCor® ECG monitor. Devices such as these can forgo the extra hardware required by their less portable or costlier stand-alone counterparts, while at the same time gain the benefits of interconnectivity, cloud-storage, and analytics afforded by the mobile phone.

Recently, this trend of utilizing mobile add-on devices has spread to the realm of medicine, a movement known as mobile health (mHealth), as rising healthcare costs and increasing interest in personal health tracking have made point-of-care (POC) biosensors an attractive and cost-effective supplement to and replacement for the cumbersome and expensive standalone diagnostic equipment typically confined to hospitals or laboratories. Developing peripheral molecular sensors, which detect and monitor a variety of disease biomarkers, for mobile phones would enable numerous POC applications allowing doctors to conduct diagnostic tests in remote settings and individuals to run simple medical tests without visiting a lab, improving the convenience, speed, and quality of medical diagnoses. While devices exist that use a part of the mobile phone for molecular tests, such as the camera [3–8], Bluetooth [9], proprietary ports [10–12], or the audio port [13,14], our intention was to develop a platform that integrates seamlessly with the smartphone by using sensitive electrochemical detection to forgo bulky external equipment typical of optical sensing methods and reducing redundant electronics in the peripheral that already exists on the phone. By focusing on making the peripheral more closely integrated with the mobile device and easier both to manage and carry around, a platform can be developed that can be more readily adopted by individuals and can encourage and promote adherence to frequent POC monitoring and testing. Just as the portability of glucose meters have substantially improved the quality of life for those living with diabetes, more powerful POC tools that harness the advanced functionalities of the mobile phone can address other chronic illnesses that are more challenging to manage. Cystic fibrosis (CF) is one such incurable genetic disease that affects more than 70,000 people worldwide [15]. Even though there are effective treatments, CF is still a complex illness. CF patients can have varying types and severity of symptoms and are always at risk of developing serious complications such as infection or organ damage. Hence, those living with CF need frequent check-ups and testing in order to receive proper treatment and reduce the number of serious complications.

In this manuscript, we will discuss both the implementation of a novel portable power harvesting mobile phone-based electrochemical biosensor platform, which utilizes as much as the phone's functionality and hardware as possible, and testing of the device for detection of a medically relevant diagnostic biomarker, secretory leukocyte protease inhibitor (SLPI), for monitoring lung infection in CF patients. As seen in Fig. 1, in the biosensor platform, a small-form factor peripheral module plugs directly into the audio jack port of a mobile device and interfaces with disposable screen-printed electrodes functionalized with a detection molecule, such as antibodies, peptides, nucleic acids, etc., depending on the

application. Via the standard 3.5 mm audio jack, the module both powers itself by rectifying audio-band tones sent by the mobile device and communicates with the phone to conduct biomolecular tests. The user can run diagnostic tests via an on-phone application, which controls the parameters of the test, analyzes the measured data, and securely transmits the results for processing by physicians or data storage.

As with most electrochemical biosensors, this electronic module contains a potentiostat that conducts and measures electrochemical assays and typically costs from \$1,000 to \$10,000 for a laboratory grade version. There have been several low cost and portable potentiostats developed and verified previously [11–13,16–20], each with their own advantages and limitations. (A table is provided later that compares many of these devices to this work.) The novelty of our module is that it takes full advantage of the pervasiveness of mobile phones, leveraging them for their standard functionality, i.e. processing power, wireless radios, battery, display, and audio jack. This tight integration with the phone reduces the hardware requirements, minimizing the cost and size of the peripheral device. Also, this harvesting design eliminates the hassle of having to charge or replace another battery minimizing waste from battery disposal and improving the overall convenience of the device, which if implemented poorly can often discourage regular use. Finally, unlike USB or other proprietary ports, the audio jack is widely used across different makes, models, and generations of mobile devices making this module hardware compatible with most platforms with an audio port.

2. Material and Methods

2.1. Mobile Phone-Based Electrochemical Biosensor Platform

The overall design of the electronic module for the biosensor platform is an updated and improved version based on our previously published work [21]. Since prior publications explain the development of the predecessor in detail, we will only briefly summarize how the device works and focus more on the enhancements and innovations we have added since.

The three main blocks of the electronic module are: the power harvester, the potentiostat for accurate and low-power cyclic voltammetry measurements, and the communication interface between the host and the module. All three of these blocks are designed to contend with the unique circuit challenges that arise from interfacing with the four connections of the audio port (left audio channel for power, right audio and microphone channels for communication, and common tied to ground), which unfortunately is AC coupled, preventing the module from directly tapping into both the phone's DC power and its analog to digital converter. The power harvester, using an augmented topology based on the University of Michigan's Project Hijack, must efficiently rectify a variable frequency tone on the left audio channel and create a regulated power supply [22]. The potentiostat, which typically must generate low frequency signals (25 mV/s triangular waves) for cyclic voltammetry, uses less computationally intensive methods to both produce the stimulus and measure the response from the sensors. Finally, the communication protocol, which allows for standardized two-way data transmission to any host device, is designed to be reliable and simple enough to run on low-power microcontrollers.

A 1.5 by 2.5-inch printed circuit board (PCB) prototype was built (Fig. 2), and costs less than \$20. This prototype was used to verify the functionality of the different blocks as well as run actual chemical tests. The design considerations for each block, as well as their performance as measured with this PCB, will be discussed in the following sections.

2.1.1. Efficient Power Harvesting from the Audio Port—The power harvester topology first steps up the low amplitude voltage tone (< 200 mV) provided by the phone with a transformer (LPR6235-123QMR from Coilcraft Inc.). The tone is then rectified by a differential-drive CMOS rectifier (comprised of ZXM61N03FTA and ZXM61P03FTA from Diodes Incorporated) and passed through a Schottky diode (DFLS120L-7 from Diodes Incorporated). Afterwards, a DC-DC converter (LTC3632EMS8E Linear Technology) drops this supply voltage to 4 V. This topology has been shown to achieve an efficiency of approximately 50% when directly coupled to an iPhone 3GS [22]. The inefficiency originates from the fact that the frequency of optimum power transfer, at which the input impedance of the harvester matches the phone's output impedance, is higher than 22 kHz, which is beyond the limit of what most phones can output through the headphone port, thus leading to poor matching. Since the 3GS has high enough available power, it can still power the module even with this mismatch. Unfortunately, as seen when testing a set of the most popular smartphones, different makes and models of phones have very diverse audio output characteristics with power available varying from 3–80 mW and output impedances ranging from 2–4 Ω [23]. Hence, correct matching is crucial for phones that have lower available power and cannot afford to lose a majority of it in an inefficient harvester. Furthermore, in order to make the device usable with all types of phones, it must be able to adapt automatically to obtain sufficient harvested power regardless of the phone and its impedance. Thus, an adjustable impedance matching network is added to the harvester to be able to achieve high efficiency and allow it to adjust its input impedance to match that of different phones.

The augmented impedance matched power harvester design is shown in Fig. 3a. By introducing an L-match network after the transformer, the resonant frequency point, which was originally outside the audio band, can be shifted down to an achievable frequency near 10 kHz (Fig. 3b). Once in this approximate range, the impedance of the network can be tuned to match the smartphone's output impedance by adjusting the frequency of phone's output signal (Fig. 3c). Using this tunable matching network and an iPhone 4, which is adjusted to have an output frequency of 15 kHz, an efficiency increase of the harvester from 47% (without the matching network) to 79% (matched) was measured.

To avoid having to set the frequency manually for every phone, an automated tuning algorithm is implemented on the device as shown in Fig. 3a [23]. All the circuit blocks on the module are power gated such that, initially, only the microcontroller is operational. The microcontroller then switches on a resistive load at the output of the harvester network. The node on the output of the rectifier is connected to the microcontroller's internal analog-to-digital converter (ADC) through a voltage divider to prevent measuring potentials higher than the supply voltage. The phone then sweeps the input frequency sent to the device with the microcontroller reporting back the attenuated output voltage of the rectifier. Since the load is constant, the frequency at which the maximum output voltage of the rectifier is

measured corresponds to the point of maximum power delivered. Using a binary search, the algorithm repeats this frequency adjustment process until the maximum voltage point is found. Once enough power is available, the other blocks can be enabled and the process repeated in order to compensate for the small impedance change caused by the increased load current. This two-step iterative process takes less than 2 seconds and ensures that the maximum power transfer point is found without creating startup issues, such as when the initial frequency is so far off of the maximum that it cannot power the entire circuit.

2.1.2. Low Power Potentiostat—The potentiostat (Fig. 4), similar to designs found in other biosensors [24,25], applies a voltage signal between the working electrode (WE) and the reference electrode (RE) of the sensor with the counter electrode (CE) supplying the required current and measures the resulting current in the WE. This potentiostat [21] specifically runs cyclic voltammetry so the stimulus is a triangular waveform. Due to the fact that the audio jack is AC coupled, thus prohibiting the module from receiving the waveform directly from the phone, an integrator (OPA333AMDBVREP from Texas Instruments) and the microcontroller's (PIC16F690 from Microchip Technology) dedicated pulse width modulation (PWM) hardware are used (Fig. 4a). To generate a ramp, the microcontroller only needs to set the duty cycle the PWM generator once rather than constantly updating an external digital-to-analog converter keeping the computational burden low during the test, thereby reducing power consumption and freeing up clock cycles to allow for drift correction. The current output signal is then measured with a resistive feedback transimpedance amplifier (TIA) as shown in Fig. 4b and illustrated in more detail in the supplementary [16,26,27]. Since the performance of the amplifier used for the TIA directly affects the accuracy and sensitivity of the potentiostat, an operational amplifier (AD8551ARMZ from Analog Devices) was selected based on its balance of low input bias current, low current noise, and power consumption. Since this potentiostat only has a single sensitivity setting, the feedback resistor value in the TIA must be selected beforehand for the range of currents expected when measuring the possible biological concentrations of the desired analyte. For the particular SLPI assay discussed in this work, a gain of 10 k Ω is used. While the fixed gain does limit the dynamic range, this design avoids both the increased power consumption of adding a second adjustable gain stage and the additional input current leakage of implementing a variable feedback resistor with switches. Furthermore, this high sensitivity design with low current leakage and low noise is able to achieve a large enough dynamic range (96 dB) to measure a particular assay without having to change the gain resistor. The buffer (AD8603AUJZ-REEL7 from Analog Devices) for the reference electrode was chosen for its very low input bias current to reduce voltage errors in the potential applied between RE and WE, and the amplifier for CE (OPA333AMDBVREP from Texas Instruments) was selected to be able to supply enough current for the entire electrochemical cell.

2.1.3. Interface with Mobile Phone—For communication across the audio port, the high resolution ADC of the phone's microphone is utilized to avoid adding an ADC to the module. To get the raw analog data from the potentiostat to the phone past the AC coupling, a voltage controlled oscillator (VCO) (ICM7555 from Intersil) is used to frequency modulate the output of the TIA. The magnitude of the VCO gain is 2.123 kHz/V with an

offset of 11.6 kHz. The monotonic range is roughly from 1–4 volts, while the approximate linear range spans about 2 volts centered around 2.4 volts. Demodulation and recovery of the data is pushed to the digital domain to be handled easily by the phone's powerful processor performing a Fast Fourier Transform (FFT) on 100 ms windows of the data stream (Fig. 5a). Brief 1 kHz tones from the microcontroller are used to correctly form the resulting voltammogram.

While the measured data from the sensor is an analog signal, digital communication between the phone and the microcontroller with RS232 over the audio port is used in order to setup the parameters for different tests. Since the parameters are set before tests are run, a high data throughput using this type of communication is not necessary. A packet, following the structure illustrated in the supplemental (Fig. A.4), is sent over RS232 at a baud rate of 2,400 baud directly on the right audio output channel to the hardware UART on the microcontroller (Fig. 5b). Once the microcontroller error checks the packet and reads the data, it sends the appropriate response back to the phone on the microphone channel. Depending on the type of mobile phone used, there can exist drift on the signal recorded by the microphone channel. While other digital communication schemes such as Manchester encoding or frequency shift keying (FSK) might be used to mitigate drift issues or improve reliability, the current packet implementation can still be deciphered with high reliability on the phone side. Essentially, instead of increasing the number of clock cycles and putting the burden on the microcontroller by adding extra decoding and encoding capabilities, the issue is pushed to the phone, which, with its superior signal processing power, can easily decipher the packet even in the presence of attenuation.

To begin using the biosensor, once the device is plugged into the headphone jack, the user opens the smartphone application. The smartphone app starts powering on the device and initiating the communication handshake between the phone and module. Concealed to the user, the smartphone supplies a 15 kHz tone on the left output channel and queries the device for its identification number. The phone sends this query wrapped in a packet structure complete with an 8-bit cyclic redundancy check (CRC) over the left audio output and immediately begins recording for a set amount of time on the microphone channel awaiting the module's response. If no response or proper packet is received or if this is the first time that this device has been linked to the particular smartphone, the phone can run the power tuning algorithm to sweep the input frequency of the rectified tone to provide optimal power to the device. After determining the optimal tone frequency, the user has the ability to select a particular electrochemical test. Depending on the desired test, the phone then sends another packet to the module informing the microcontroller of the voltage range (up to ± 2 V) and scan rate (25, 50, or 100 mV/s) to use. The module replies confirming that it received the set message as it powers on the potentiostat and sets the working electrode voltage to the initial potential. Once ready, the application enables the start button so that the user can begin the test. After receiving the start command from the phone, the digital communication is ceased and frequency modulated data from the potentiostat is transferred back to the phone. Afterwards, on the smartphone side, the data is demodulated and aligned with the voltage input waveform creating the voltammogram to be displayed and saved.

2.2. Materials

In addition to functional and characterization tests, the prototype device was used to run electrochemical experiments and assays. For all experiments, the gold electrodes were cleaned first with a 3:1 mixture of 50 mM KOH (P250–500) and H₂O₂ (H325–500) from Fisher Scientific for 10 minutes and then with a cyclic voltammetry sweep with H₂SO₄ [28]. Washing steps during the functionalization process involve rinsing the electrodes with Phosphate Buffered Saline (PBS) and drying with air.

2.2.1. Electrochemical Verification—Cyclic voltammetry experiments were conducted using an equal mixture of potassium ferrocyanide (K₄[Fe(CN)₆]) and potassium ferricyanide (K₃[Fe(CN)₆]) from Spectrum (P1286, P1296) in a phosphate buffer solution of 150 mM potassium phosphate monobasic from Fischer Scientific (P285–500) and potassium phosphate dibasic from EMD Millipore (PX1570-1). The biosensor module was connected to the audio port of a PC, which controls the parameters of the electrochemical test via the right audio channel and processes the recorded data. Samples of 62.5 μM, 125 μM, 250 μM, and 500 μM K₄[Fe(CN)₆] / K₃[Fe(CN)₆] were applied to gold screen-printed electrodes (SPE) from DropSens (DRP-250AT). Cyclic voltammetry using a sweep from -140 mV to 380 mV and scan rate of 25 mV/s was run on both the proposed mHealth biosensing platform and a commercial 750E potentiostat from CH Instruments, Inc.

2.2.2. SLPI Assay—Gold DropSens electrodes were functionalized for detection of SLPI. 50 μg/ml of anti-human SLPI (R&D Systems MAB1274) were mixed with Traut's reagent (Pierce 26101) and dropped on the gold working electrodes and incubated overnight at -4°C. 2% BSA (Thermo Scientific 37525) was applied for 1 hour at room temperature to block the surface. Afterwards, various concentrations of SLPI (R&D 1274-PI) in 20 μL droplets were added to each electrode before adding the secondary antibody (GenWay Biotech GWB-8AD57A) and then the NeutrAvidin conjugated alkaline phosphatase (Thermo Scientific 31002). Each binding step lasts an hour and includes washing in between. Finally, before running cyclic voltammetry on each electrode, the substrate, p-AminoPhenyl Phosphate (Santa Cruz Biotechnology sc-281392) is added and allowed to react for 10 minutes. The sweep range and scan rate are -200 mV to 300 mV and 25 mV/s, respectively.

3. Results and Discussion

3.1. Potentiostat Module Performance

We first characterized the electrical performance of the biosensing module. The noise of the potentiostat's TIA with the gain set at 100 kΩ was measured using a signal analyzer (Agilent 35670A). This measurement setup was also used to determine the frequency response (160 Hz cutoff frequency) in addition to the output power spectrum. From this measurement, the input referred total integrated current noise for a 1 kHz bandwidth was calculated to be 216 pA_{RMS}. Hence, this potentiostat with a standard resistive feedback TIA topology is able to measure a bidirectional current from ±300 pA to ±20 μA (96 dB dynamic range) with a 100 kΩ gain. The peak power consumption while running tests is 6.9 mW with the potentiostat

and microcontroller dominating the power budget (Fig. 6), which, with the tuned matching network, can be harvested from the smartphone.

3.2. Verification with Laboratory Grade Equipment

Ferro/Ferri is a commonly used reversible redox pair when running electrochemical experiments due to its stability and distinctive voltammogram shape. As seen in Fig. 7, the measured voltammogram of the device matches well with that of the CHI potentiostat given that variations will occur due to the tests being run at different times on the same electrode. When comparing the features extracted from the CHI data with those from the device, the peak currents vary less than 2% and the redox potentials differ by only 6 mV. The measured redox potential of 150 mV (versus an Ag pseudo reference electrode) also matches well with similar experiments in literature [29].

3.3. Biomarker Assay

Sandwich assays, similar to enzyme linked immunosorbent assays (ELISA), are a commonly used technique to detect biomarkers (Fig. 8a). First, antibodies are immobilized on the electrode surface with a cross-linker and blocker. Then the test sample is applied to the electrode and the target antigen is allowed to bind to the immobilized antibody. The secondary antibody with an attached enzyme is introduced and binds to the captured antigen. Then, by adding a substrate that the enzyme can convert to a redox active molecule, an amplified electrochemical signal proportional to the concentration of the target biomarker can be measured.

In this paper, an assay for SLPI has been developed and tested with the electronic module for use in tracking lung infections in CF patients. SLPI is a biomarker that plays anti-microbial and anti-inflammatory roles within the body. It has been shown that decreased levels of SLPI in sputum, the mucus coughed out of the lungs of individuals with CF, indicates a *Pseudomonas aeruginosa* infection, which can be serious and often fatal [30]. When coupled with the proposed POC molecular sensor, this biomarker allows for frequent testing and can give the user and physician early alerts of dangerous infections. The concentration of SLPI found in a normal and infected CF lung is 11 ± 5 nM and 3.99 ± 2 nM, respectively [30]. Fig. 8b shows a set of CV curves of different concentrations obtained by the device. The corresponding calibration plot of the peak currents (Fig. 8c) was determined through repeated measurements ($N=3$) of each electrode for every concentration. As seen from this curve, SLPI can be detected at these diagnostically relevant concentrations and, hence, would be useful as a biosensor for diagnosing infection and monitoring CF.

3.4. Platform Comparison

These chemical tests have shown this device to perform at least as well as prior POC electrochemical biosensors in terms of biosensing functionality. To highlight both the differences and improvements of this platform, Table 1 shows a comparison of our device with other portable sensing platforms previously reported in literature. It is important to note that while the limit of detection (LOD) of the analytes specified in the table can be used as approximate indicators of the sensitivity of the biosensor, these numbers cannot be directly compared to one another since different analytes not only vary in physical characteristics

such as size, shape, and charge, but also often require uniquely different assays in order to achieve specificity. Furthermore, even when comparing devices measuring the same analyte, the type of transducers (size, material, geometry, etc.), methods of functionalization (reagents, antibodies, enzymes, etc.), and how the sample is handled (isolating, mixing, use of microfluidics, etc.) can vastly affect the biosensors' overall limit of detection. Hence, due to this distinction and the fact that our work focuses mainly on improvements made in terms electronic sensing module, this discussion will mostly emphasize the similarities and differences of the electronic device aspect of these biosensors, rather than optimizations made on the biological and sample handling side.

Each of the devices listed here lies somewhere on the wide spectrum of POC applications ranging from handheld replacements for benchtop potentiostats to compact wearable biosensors. Firstly, [16] and [17] are both low-cost portable potentiostats meant to be paired with a PC and run on either USB or an external power supply. These devices demonstrate that potentiostats can be made relatively inexpensively and built into a manageable size when compared to full-featured versions commonly found in laboratories. Since external sources supply power to these devices, low-power consumption of the circuitry is not as crucial and, as partly illustrated in the table, they tend to have more functionality and versatility than the other devices, such as being able to run a variety of different electrochemical techniques. However, these devices are costlier than the other more portable biosensors listed and also require interfacing with a PC, restricting their point-of-care usefulness. As a direct comparison, [11] and [12] use modules that instead connect to a PDA and a smartphone respectively, via the USB port taking advantage of the phone's processing power and connectivity. As with all the other mobile-based devices, this smartphone oriented design costs less and has a size more compatible with portable everyday use. Unfortunately, USB is not compatible with across all smartphone versions and requires extra hardware to implement the interface.

Hence, another wave of devices [13,14,31], as well as our own device, has sought to take advantage of the headphone jack, which is the one standardized port across all currently available smartphones and some feature phones as well. Bluetooth, used in [9,32], is another communication method that can be found in most new mobile devices. The major benefits of Bluetooth are the higher data rate (270 kbps using Bluetooth Low Energy compared to <2 kbps in this work) and the ability to physically separate the electronic module from the phone, which is especially advantageous for wearable applications [32]. However, other than for continuous or wearable monitoring, it can be argued that the benefits of adding Bluetooth in many POC biosensing applications do not outweigh the costs. As the headphone jack based biosensors in the table have proven, most electrochemical sensing techniques such as cyclic voltammetry, chronoamperometry, and step voltammetry, are generally very slow measurements and do not require the much higher bandwidths that Bluetooth provides at the expense of higher power consumption and a battery additional to the phone's. Furthermore, for periodic daily or weekly testing, there is no clear benefit for the user to be able to have a dongle separate from the smartphone as the phone itself is already portable. However, the primary advantage of the headphone interface is that the electronic module does not have to conform to either the USB or Bluetooth communication standards and can avoid adding dedicated components, Bluetooth chip or USB host shield, along with the processing

overhead required on the device side. Instead, a simple RS232 or FSK communication method can be set up and, as demonstrated with our device, the digitization of the analog signal can be pushed to the smartphone further reducing the high power and high cost components needed on the module itself. The fact that the headphone-based biosensors in the table have a slightly lower approximate costs is an indicator of the increased complexity brought on by Bluetooth, which for our particular biosensing application, is not beneficial. Finally, while all the other electrochemical biosensors using the headphone jack have batteries, our device is able to harvest its power directly from the smartphone. While these batteries offer enough power to perform more types of tests [13] as well as implement more intensive techniques [9], we have shown that harvesting power from the headphone port is enough to implement a CV based biosensor with comparable sensitivity. Furthermore, power harvesting eliminates the hassle of having to either replace or charge a battery in addition to the phone's battery improving user convenience for periodic use.

4. Conclusions

We have implemented a complete mobile phone-based electrochemical biosensor platform that uses the audio jack on a smartphone for both communication and power. The design of the prototype focuses on reducing the size and cost of the external device and using all the resources provided by smartphones, especially those features introduced by the advances in smartphone technology. Due to its full utilization of the headphone port, it has excellent cost and sensitivity, comparable to that of the state of the art. Furthermore, all the other electrochemical detection platforms discussed, still require either an external power source or additional battery, which can be bulky and cumbersome for POC use, unlike the harvesting design presented in this work. The prototype, complete with an automatic tunable matching network, is within the power budget of most commercially available smartphones. We have also shown that this POC platform not only can produce voltammograms that match well with the data measured from a table top potentiostat, but also be used in assays to detect a diagnostically relevant biomarker, SLPI, to help improve the quality of life for CF patients.

Supplementary Material

Refer to Web version on PubMed Central for supplementary material.

Acknowledgments

This work was partially supported by the Qualcomm Institute summer undergraduate research scholars program and the National Institutes of Health, Grant UL1TR000100. The content is solely the responsibility of the authors and does not necessarily represent the official views of the NIH.

Abbreviations

SLPI	secretory leukocyte protease inhibitor
CF	cystic fibrosis

References

1. Kim J, Zhang W, Nyonyitono M, Lourenco L, Nanfuka M, Okoboi S, et al. Feasibility and acceptability of mobile phone short message service as a support for patients receiving antiretroviral therapy in rural Uganda: a cross-sectional study. *J. Int. AIDS Soc.* 2015; 18
2. [accessed May 30, 2014] Smartphone Users Worldwide Will Total 1.75 Billion in 2014. (n.d.) <http://www.emarketer.com/Article/Smartphone-Users-Worldwide-Will-Total-175-Billion-2014/1010536>
3. McGeough CM, O'Driscoll S. Camera Phone-Based Quantitative Analysis of C-Reactive Protein ELISA. *IEEE Trans. Biomed. Circuits Syst.* 2013; 7:655–659. [PubMed: 24232626]
4. Cevenini L, Calabretta MM, Tarantino G, Michelini E, Roda A. Smartphone-interfaced 3D printed toxicity biosensor integrating bioluminescent “sentinel cells”. *Sens. Actuators B Chem.* (n.d.).
5. Su K, Zou Q, Zhou J, Zou L, Li H, Wang T, et al. High-sensitive and high-efficient biochemical analysis method using a bionic electronic eye in combination with a smartphone-based colorimetric reader system. *Sens. Actuators B Chem.* 2015; 216:134–140.
6. Xu W, Lu S, Chen Y, Zhao T, Jiang Y, Wang Y, et al. Simultaneous color sensing of O₂ and pH using a smartphone. *Sens. Actuators B Chem.* 2015; 220:326–330.
7. Berg B, Cortazar B, Tseng D, Ozkan H, Feng S, Wei Q, et al. Cellphone-Based Hand-Held Microplate Reader for Point-of-Care Testing of Enzyme-Linked Immunosorbent Assays. *ACS Nano.* 2015; 9:7857–7866. [PubMed: 26159546]
8. Ludwig SKJ, Tokarski C, Lang SN, van Ginkel LA, Zhu H, Ozcan A, et al. Calling Biomarkers in Milk Using a Protein Microarray on Your Smartphone. *PLoS ONE.* 2015; 10:e0134360. [PubMed: 26308444]
9. Zhang D, Lu Y, Zhang Q, Liu L, Li S, Yao Y, et al. Protein detecting with smartphone-controlled electrochemical impedance spectroscopy for pointof-care applications. *Sens. Actuators B Chem.* 2016; 222:994–1002.
10. Doeven EH, Barbante GJ, Harsant AJ, Donnelly PS, Connell TU, Hogan CF, et al. Mobile phone-based electrochemiluminescence sensing exploiting the “USB On-The-Go” protocol. *Sens. Actuators B Chem.* 2015; 216:608–613.
11. Ionescu, C.; Svasta, P.; Tamas, C.; Bala, C.; Rotariu, L. Portable measuring and display unit for electrochemical sensors; *Des. Technol. Electron. Packag. SIITME 2010 IEEE 16th Int. Symp. For;* 2010. p. 215-218.
12. Lillehoj PB, Huang M-C, Truong N, Ho C-M. Rapid electrochemical detection on a mobile phone. *Lab. Chip.* 2013; 13:2950–2955. [PubMed: 23689554]
13. Nemiroski A, Christodouleas DC, Hennek JW, Kumar AA, Maxwell EJ, Fernández-Abedul MT, et al. Universal mobile electrochemical detector designed for use in resource-limited applications. *Proc. Natl. Acad. Sci.* 2014; 111:11984–11989. [PubMed: 25092346]
14. Wang X, Gartia MR, Jiang J, Chang T-W, Qian J, Liu Y, et al. Audio jack based miniaturized mobile phone electrochemical sensing platform. *Sens. Actuators B Chem.* 2015; 209:677–685.
15. Ramsey BW, Davies J, McElvaney NG, Tullis E, Bell SC, D evínek P, et al. A CFTR Potentiator in Patients with Cystic Fibrosis and the G551D Mutation. *N. Engl. J. Med.* 2011; 365:1663–1672. [PubMed: 22047557]
16. Rowe AA, Bonham AJ, White RJ, Zimmer MP, Yadgar RJ, Hobza TM, et al. CheapStat: An Open-Source, “Do-It-Yourself” Potentiostat for Analytical and Educational Applications. *PLoS ONE.* 2011; 6:e23783. [PubMed: 21931613]
17. Cruz AFD, Norena N, Kaushik A, Bhansali S. A low-cost miniaturized potentiostat for point-of-care diagnosis. *Biosens. Bioelectron.* 2014; 62:249–254. [PubMed: 25016332]
18. Huang C-Y, Lin H-Y, Wang Y-C, Liao W-Y, Chou T-C. A portable and wireless data transmission potentiostat. *2004 IEEE Asia-Pac. Conf. Circuits Syst. 2004 Proc.* 2004; 2:633–636.
19. Huang, C-Y.; Lee, M-H.; Wu, Z-H.; Tseng, H-Y.; Huang, Y-C.; Liu, B-D., et al. A Portable Potentiostat with Molecularly Imprinted Polymeric Electrode for Dopamine Sensing; *IEEE Circuits Syst. Int. Conf. Test. Diagn. 2009 ICTD 2009;* 2009. p. 1-4.
20. Blanco, JR.; Ferrero, FJ.; Campo, JC.; Anton, JC.; Pingarron, JM.; Reviejo, AJ., et al. Design of a Low-Cost Portable Potentiostat for Amperometric Biosensors; *Proc. IEEE Instrum. Meas. Technol. Conf. 2006 IMTC 2006;* 2006. p. 690-694.

21. Sun, A.; Wambach, T.; Venkatesh, AG.; Hall, DA. A low-cost smartphone-based electrochemical biosensor for point-of-care diagnostics; 2014 IEEE Biomed. Circuits Syst. Conf. BioCAS; 2014. p. 312-315.
22. Kuo Y-S, Schmid T, Dutta P. Hijacking power and bandwidth from the mobile phone's audio interface. Proc Int Symp Low Power Electron. Des. 2010
23. Yao, Chengyang; Sun, Alexander; Hall, Drew A. Efficient Power Harvesting from the Mobile Phone Audio Jack for mHealth Peripherals. Seattle, WA: 2015.
24. Vergani M, Carminati M, Ferrari G, Landini E, Caviglia C, Heiskanen A, et al. Multichannel Bipotentiostat Integrated With a Microfluidic Platform for Electrochemical Real-Time Monitoring of Cell Cultures. IEEE Trans. Biomed. Circuits Syst. 2012; 6:498–507. [PubMed: 23853236]
25. Li L, Liu X, Qureshi WA, Mason AJ. CMOS Amperometric Instrumentation and Packaging for Biosensor Array Applications. IEEE Trans. Biomed. Circuits Syst. 2011; 5:439–448. [PubMed: 23852176]
26. Hwang S, Sonkusale S. CMOS VLSI Potentiostat for Portable Environmental Sensing Applications. IEEE Sens. J. 2010; 10:820–821.
27. Ramfos I, Vassiliadis N, Blionas S, Efstathiou K, Fragoso A, O'Sullivan CK, et al. A compact hybrid-multiplexed potentiostat for real-time electrochemical biosensing applications. Biosens. Bioelectron. 2013; 47:482–489. [PubMed: 23624017]
28. Fischer LM, Tenje M, Heiskanen AR, Masuda N, Castillo J, Bentien A, et al. Gold cleaning methods for electrochemical detection applications. Microelectron. Eng. 2009; 86:1282–1285.
29. Ferreira AAP, Fugivara CS, Barrozo S, Suegama PH, Yamanaka H, Benedetti AV. Electrochemical and spectroscopic characterization of screen-printed gold-based electrodes modified with self-assembled monolayers and Tc85 protein. J. Electroanal. Chem. 2009; 634:111–122.
30. Weldon S, McNally P, McElvaney NG, Elborn JS, McAuley DF, Wartelle J, et al. Decreased Levels of Secretory Leucoprotease Inhibitor in the Pseudomonas-Infected Cystic Fibrosis Lung Are Due to Neutrophil Elastase Degradation. Immunol. J. 2009; 183:8148–8156.
31. Laksanasopin T, Guo TW, Nayak S, Sridhara AA, Xie S, Olowookere OO, et al. A smartphone dongle for diagnosis of infectious diseases at the point of care. Sci. Transl. Med. 2015; 7:273re1–273re1.
32. Gao W, Emaminejad S, Nyein HYY, Challa S, Chen K, Peck A, et al. Fully integrated wearable sensor arrays for multiplexed in situ perspiration analysis. Nature. 2016; 529:509–514. [PubMed: 26819044]

Biographies

Alexander Sun received his B.S. degree in 2012 in Electrical Engineering and Computer Science from the University of California, Berkeley and his M.S. degree in 2014 in Electrical and Computer Engineering from the University of California, San Diego where he is currently pursuing a PhD. His research focus is on electrochemical biosensors, electrochemical measurement techniques, and compact, low power circuit design for biomedical and point-of-care devices.

Chengyang Yao obtained his Bachelor degree in Electrical Engineering from University of California, San Diego. At present, he is pursuing a PhD from Stanford University. His research activities focus on biomedical devices and biochips.

A.G. Venkatesh received the B.Sc. degree in Biochemistry from Madras University - India, M.Sc. degree in Biotechnology from Bharathidasan University - India, M.Tech. degree in Bioelectronics from Tezpur University - India, and Ph.D. in Physics from Bielefeld University - Germany.

During his doctoral research, he developed a novel platform to monitor DNA-Protein interactions in real-time and as a postdoctoral researcher at University of Freiburg - Germany, he developed low cost smartphone-based devices for biomedical applications.

Currently at the University of California, San Diego, he is involved in developing smartphone-based electrochemical sensors for point-of-care application.

Drew A. Hall received the B.S. degree in computer engineering with honors from the University of Nevada, Las Vegas, NV, USA, in 2005, and the M.S. and Ph.D. degrees in electrical engineering from Stanford University, Stanford, CA, USA, in 2008 and 2012, respectively.

From 2011 to 2013, he worked as a research scientist at the Intel Corporation in the Integrated Biosensors Laboratory. Since 2013, he has been with the University of California at San Diego as an Assistant Professor in the Department of Electrical and Computer Engineering. His research interests include bioelectronics, biosensors, analog circuit design, medical electronics, and sensor interfaces.

Highlights

- Device plugs into audio port of mobiles transforming them into molecular sensors.
- Can efficiently harvest its power (79% efficiency) from mobile phones.
- Measurements match well when compared to data from a benchtop potentiostat.
- Platform is able to detect SLPI in the relevant biological range for cystic fibrosis.

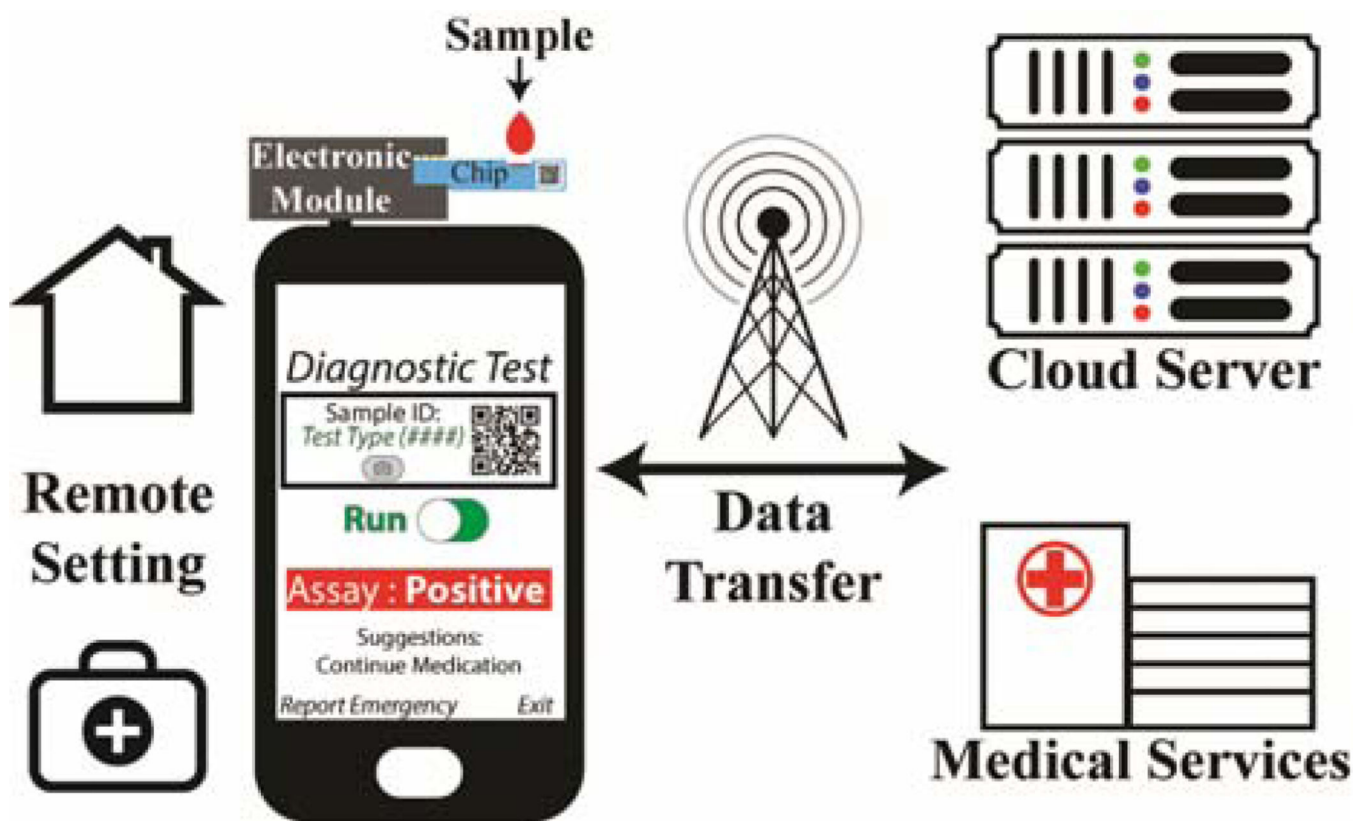


Fig. 1. Diagram of the mHealth ecosystem that combines the biosensor module, a smartphone, software application, functionalized screen-printed electrodes (SPE), and network connectivity to be used together as a point-of-care (POC) device for running diagnostic tests in remote areas or for at-home testing.

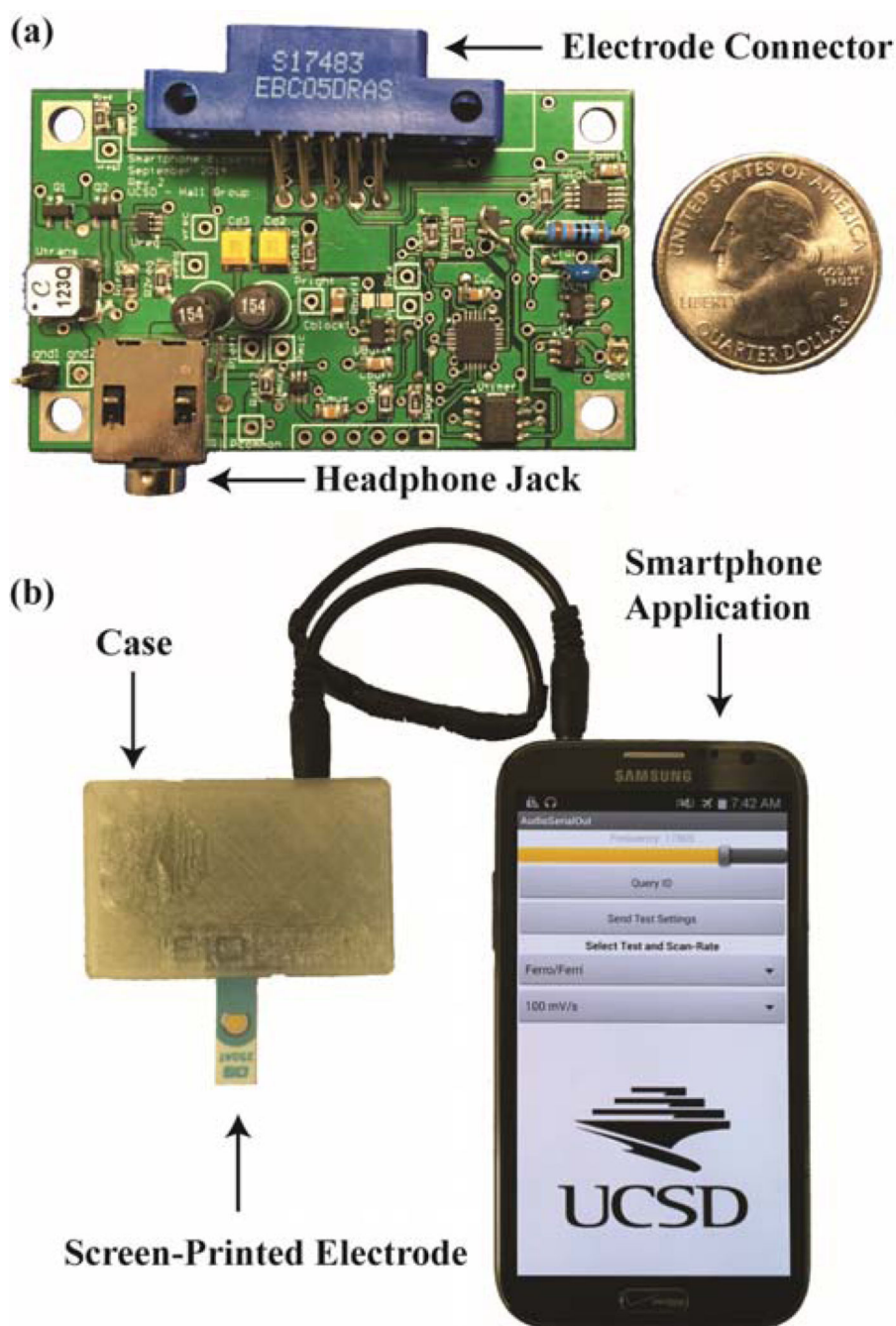


Fig. 2.
a) Photograph of the 1.5 by 2.5-inch PCB module prototype and b) the module, complete with a 3D-printed case, being powered by and communicating with a Samsung Note 2. A functionalized DropSens electrode is inserted into the edge-connector mounted on the device.

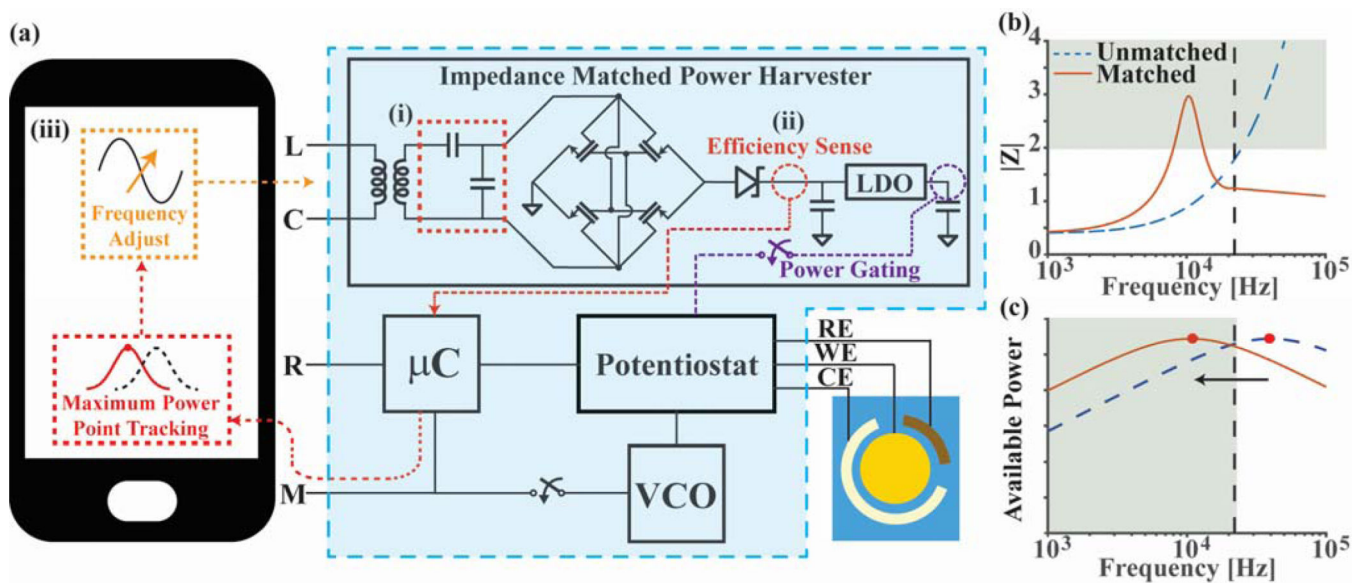


Fig. 3. (a) Simplified system schematic with smartphone, electronic module (boxed), and disposable sensor. Prior to powering the potentiostat, the device enters an “efficiency sense mode” that, through an iterative process, matches the impedance between the device and audio output of a smartphone. The harvester augmented with a matching network (i) generates the supply voltage for the entire module. The voltage output, which corresponds to the efficiency of the power transfer, can be measured (ii) by the microcontroller and then sent to the smartphone for analysis by a maximum power point tracking algorithm that adjusts the frequency of the phone’s output (iii). (b) Plot comparing the impedance seen looking into the harvester for matched and unmatched topologies. (c) Plot illustrating that the matching network can shift the maximum available power point down into the audio band to match with different types of phones.

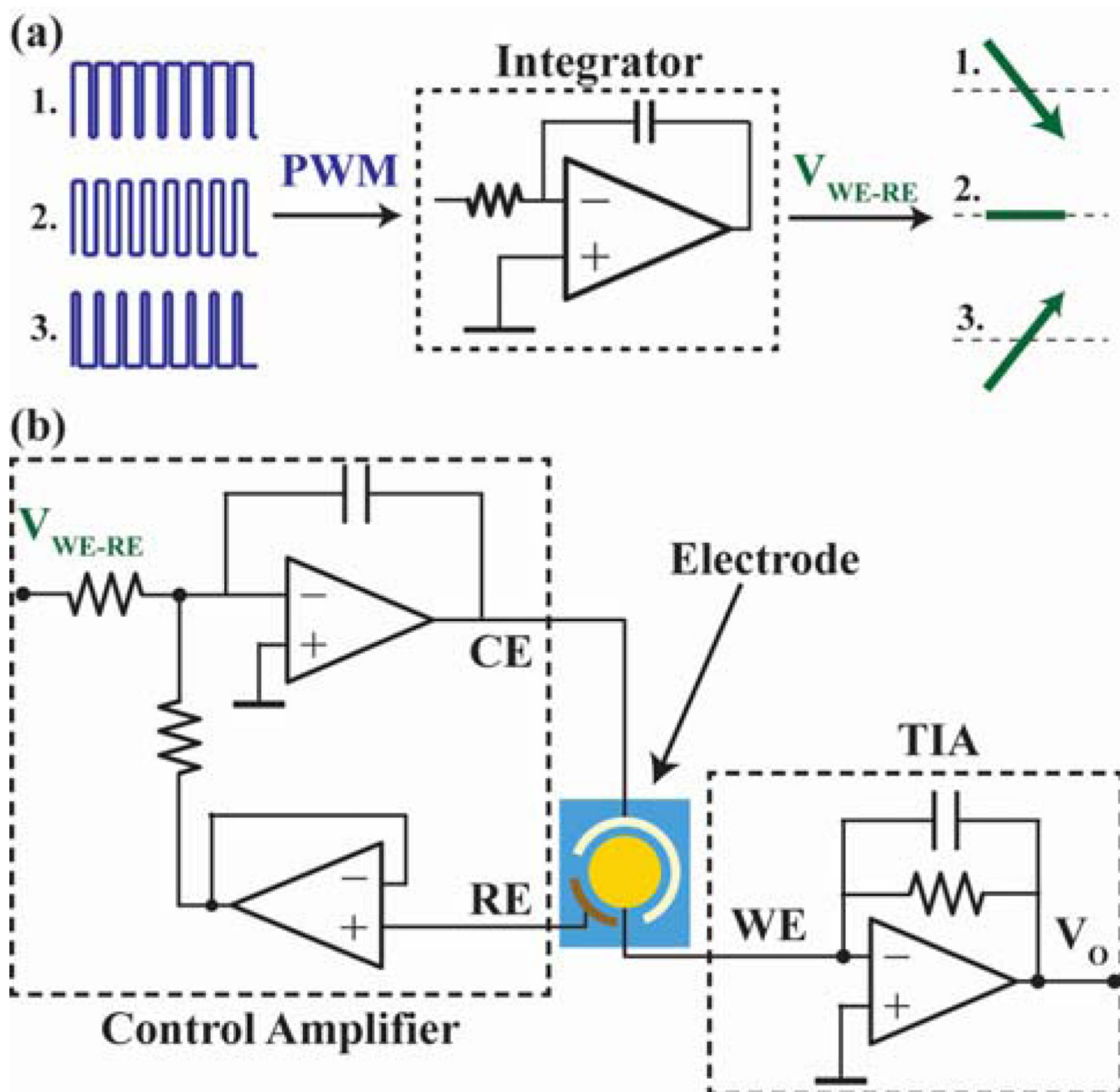


Fig. 4. Schematic of the potentiostat. (a) The microcontroller outputs a PWM signal that is integrated into either a ramp or constant voltage depending on the duty cycle. (b) The Control Amplifier block controls the voltage between the WE and the RE using this integrated signal. The TIA measures the current generated at the WE.

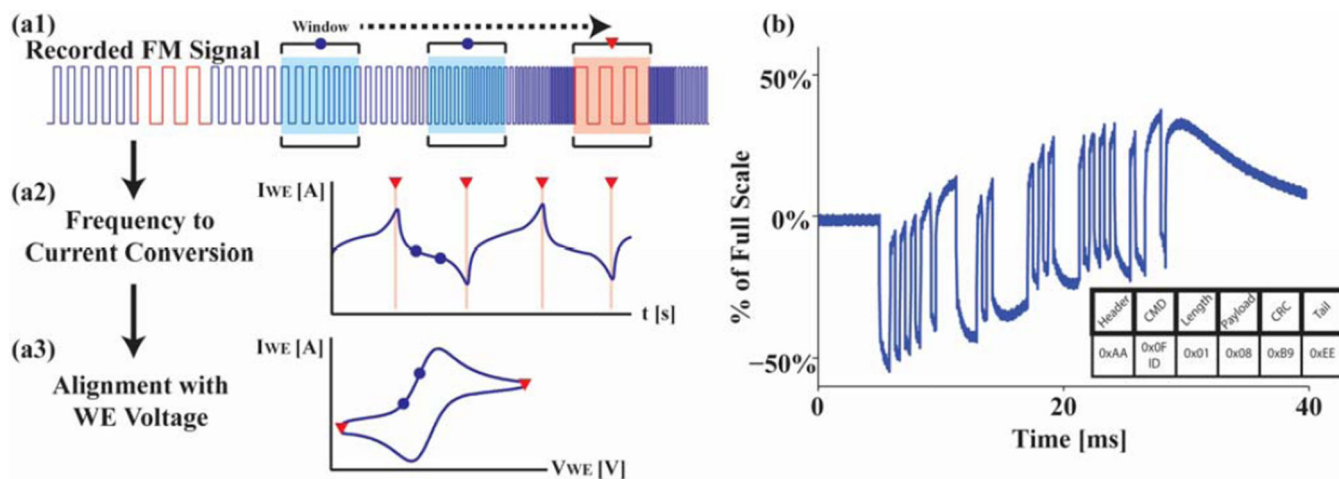


Fig. 5. The recorded frequency modulated analog signals (a1) are first partitioned into different windows of time. (a2) Each window is converted to a frequency via FFT and then transformed back into measured current. (a3) Finally, using the markers, the current is aligned with the working electrode voltage applied. (b) On the digital communication side, raw RS-232 data is directly recorded on the microphone channel sampled at 44 kHz. The decoded packet is shown below the plot.

Power Consumption (6.9 mW)

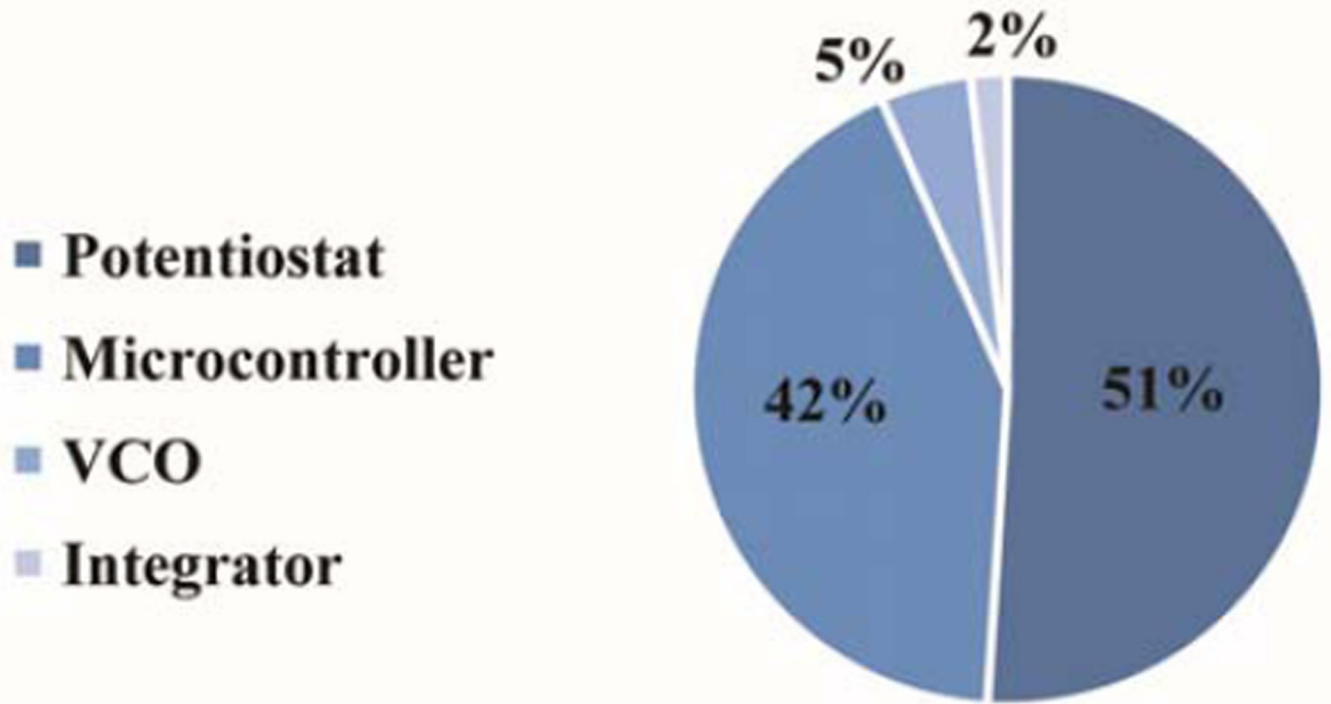


Fig. 6. System power usage per block in milliwatts excluding losses from the harvesting circuitry. While idle and awaiting a command from the phone, the module consumes 2.93 mW.

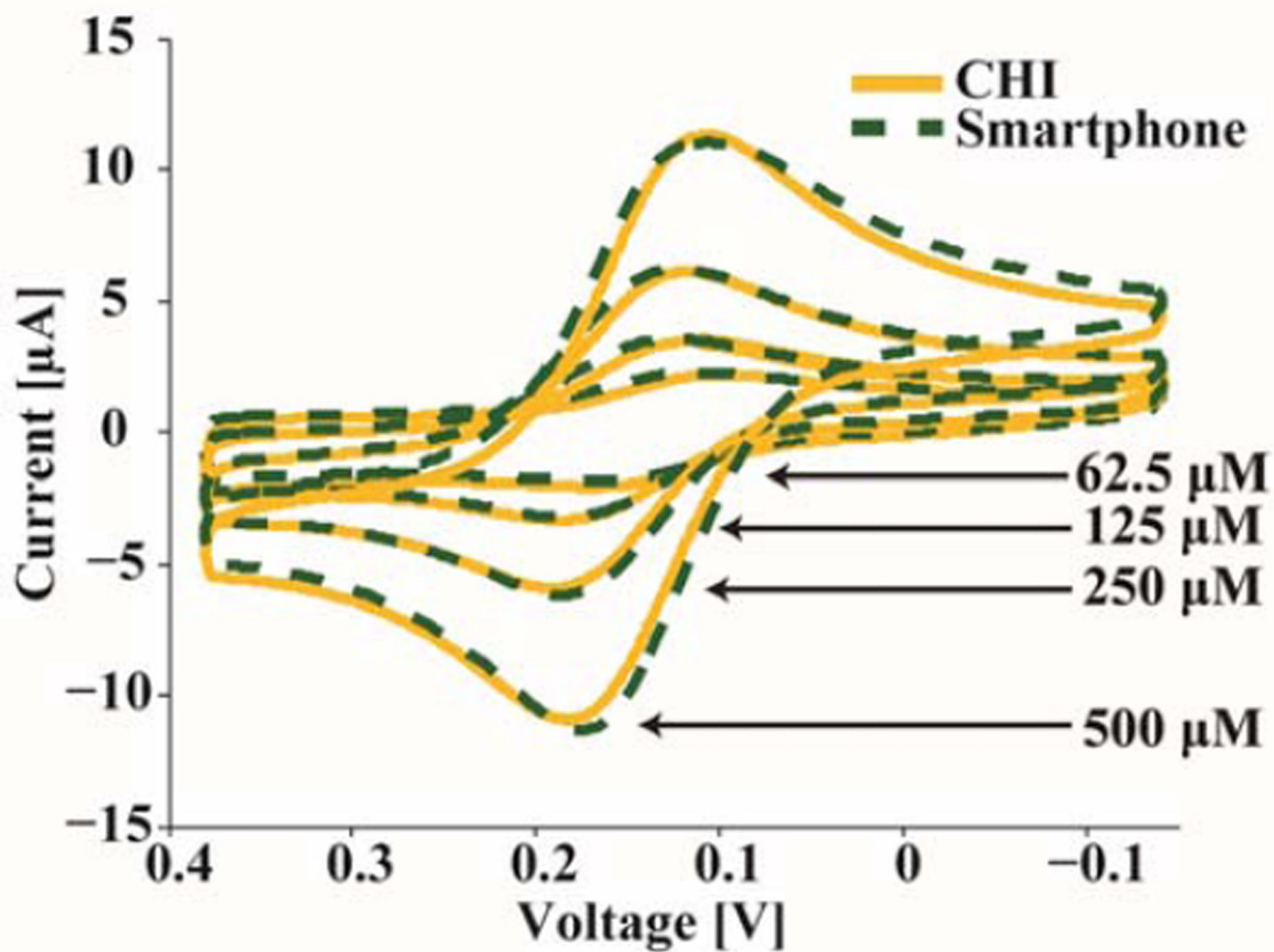


Fig. 7. Comparison between a table-top potentiostat and the mobile phone platform with varying concentrations of $(\text{K}_4[\text{Fe}(\text{CN})_6])$ and $(\text{K}_3[\text{Fe}(\text{CN})_6])$.

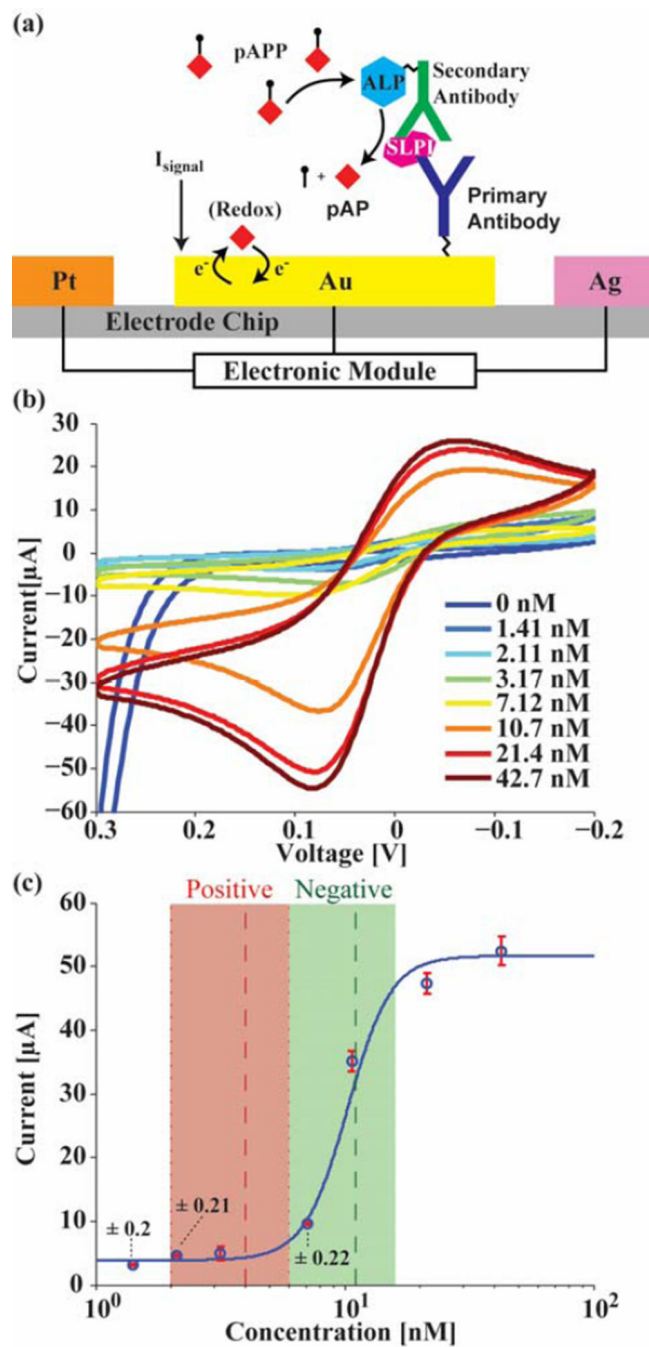


Fig. 8.
 a) Diagram of SLPI sandwich assay, b) SLPI CV curves for different concentrations, and c) the calibration curve of the results with each electrode measured in triplicate (N=3), annotated with error bars as well as the positive and negative diagnosis ranges.

TABLE 1

LITERATURE COMPARISON

Paper	Techniques	Min. Measurable Current [nA]	Analyte – LOD	Device / Connection	Power Source	Cost
Ionescu et al., [11] SHTME (2010)	CA, CV, Polarography	100	N/A	PDA / USB	External Supply	N/A
Plaxco et al., [16] PLOS ONE (2011)	CV, LSV, SWV, SV	~100	Arsenic (Water Safety) – 130 μ M	PC / USB	USB	<\$80
Lillehoj et al., [12] Lab Chip (2013)	CA	N/A	PfPRP2 (Malaria) – 432 pM	Smartphone / USB	Additional Battery	\$40 *
Bhansali et al., [17] Biosens. Bioelectron. (2014)	CV	5,000	Cortisol (Stress) – 1 pM	PC / SSH	External Supply	\$195 *
Whitesides et al., [13] PNAS (2014)	CV, CA, DPV, SWV, Potentiometry	0.5	Blood Glucose – 2.7 mM, PfPRP2 (Malaria) – 540 pM, Sodium – 100 μ M, Heavy Metals – 19 μ M	Mobile Phone / Headphone	Additional Battery	<\$25 *
Sia et al., [31] Sci. Transl. Med. (2015)	ELISA (optical)	N/A	HIV Antibody, Syphilis Antibody – N/A	Smartphone / Headphone	Harvested	\$31
Liu et al., [14] Sens. Actuator B-Chem (2015)	CV	N/A	Nitrate – 3.2 mM	Smartphone / Headphone	Additional Battery	\$10
Liu et al., [9] Sens. Actuator B-Chem (2016)	EIS	N/A	BSA – 27 nM, thrombin – 41 pM	Smartphone / Bluetooth	Additional Battery	~\$35 *
Ali et al., [32] Nature (2016)	CA, Potentiometry	1	Glucose, Lactate, Sodium, Potassium – N/A	Smartphone / Bluetooth	Additional Battery	~\$50 *
<i>This Work</i>	CV	0.3	<i>SLPI (CF) – 1 nM</i>	<i>Smartphone / Headphone</i>	<i>Harvested</i>	<i><\$20 *</i>

CA – Chronoamperometry, CV – Cyclic Voltammetry, LSV – Linear Sweep Voltammetry, SWV – Square Wave Voltammetry, DPV – Differential Pulse Voltammetry, SV – Stripping Voltammetry, EIS – Electrochemical Impedance Spectroscopy, LOD – Limit of Detection

* Calculated from BOM provided (at quantity 1000)